2000-11

JOURNAL OF GEOPHYSICAL RESEARCH, VOL. 105, NO. A9, PAGES 21,015–21,023, SEPTEMBER 1, 2000

# Anomalous cosmic ray argon and other rare elements at 1-4 MeV/nucleon trapped within the Earth's magnetosphere

J. E. Mazur,[1] G. M. Mason,[2,3] J. B. Blake,[1] B. Klecker,[4] R. A. Leske,[5] M. D. Looper,[1] and R. A. Mewaldt[5]

**Abstract.** We summarize over 6 years of observations of ~1-4 MeV/nucleon heavy ions trapped in the Earth's magnetosphere on L shells of 1.7-3. We obtained these new results in low Earth orbit with the SAMPEX spacecraft; they extend the observations of trapped heavy ions in this L range to much lower energies than had previously been examined in detail. At 1-4 MeV/nucleon we observed a trapped population with a peak intensity near L~2.3 that includes the anomalous cosmic ray species O, Ne, and Ar also observed in interplanetary space at 1 AU. We also found elements with low first ionization potential (C, Mg-S, and Fe) trapped with the same spatial distribution. The low-energy trapped population increased in intensity between 1996 and 1997, roughly during solar minimum and minimum geomagnetic activity. It is possible that the 1-4 MeV/nucleon trapped population originates from a number of sources, including high-energy trapped anomalous cosmic rays that have lost energy in the residual atmosphere in the case of O and Ne, and directly incident, singly charged anomalous cosmic rays that have become stripped and subsequently trapped in the case of Ar. The group of trapped elements with low first ionization potential (C, Mg-S, and Fe) have roughly solar wind abundances relative to one another, suggesting a possible link between this trapped component and recently discovered solar wind pickup ions released from dust grains within the inner heliosphere.

## 1. Introduction

The bulk of the anomalous cosmic rays (ACR) are a sample of the local interstellar medium. Interstellar gas atoms with first ionization potential (FIP) greater than that of H (e.g. He, N, O, Ne, and Ar) are to a large extent neutral in interstellar space, flow unimpeded into the heliosphere, and can become singly ionized from solar ultraviolet photons or through charge exchange collisions with the solar wind. Once convected out to the solar wind termination shock, these singly charged ions are a seed population for shock acceleration; they can then propagate back into the solar system as energetic ACR [e.g. *Klecker et al.* 1998]. In addition to the more abundant He, N, O, Ne and Ar, *Reames* [1999a] reported ACR-like turn-ups in the energy spectra of Mg, Si, and S below ~5 MeV/nucleon at 1 AU during 1994-1998. Low fluxes of neutral interstellar atoms may be the source for some of these rare ACR-like enhancements observed at 1 AU [*Reames* 1999a]. Carbon with charge states of +2 to +5 above 7 MeV/nucleon may have dominated the turn-up in the 1 AU C spectrum in 1992-1993 instead of singly ionized C from an inner heliospheric source [*Klecker et al.*, 1998, and references therein].

[1]Space Sciences Department, The Aerospace Corporation, El Segundo, California.

[2]Department of Physics, University of Maryland, College Park, Maryland.

[3]Also at Institute for Physical Science and Technology, College Park, Maryland.

[4]Max-Planck-Institut für Extraterrestriche Physik, Garching, Germany.

[5] Department of Physics, California Institute of Technology, Pasadena, California.



Paper number 1999JA000272.
0148-0227/00/1999JA000272$09.00

Below ~10 MeV/nucleon the bulk of the ACR are singly ionized [*Klecker et al.*, 1995, *Klecker et al.*, 1998] and can penetrate to low latitudes within the Earth's magnetosphere because of their high magnetic rigidity. *Blake and Friesen* [1977] showed that if an ACR ion loses some of its remaining electrons in a collision with the upper atmosphere, the sudden rigidity change, if sufficiently large, can lead to stable trapping and the formation of a belt of interstellar material readily accessible to spacecraft in low Earth orbit [e.g., *Grigorov et al.*, 1991; *Cummings et al.*, 1993].

The trapped ACR elemental and isotopic composition, time dependence, and spatial dependence above ~10 MeV/nucleon have been studied in detail with instrumentation onboard the SAMPEX satellite [e.g., *Selesnick et al.*, 1995a; *Looper et al.*, 1996]. *Kleis et al.* [1995] and *Barz et al.* [1995] reported trapped heavy ions in the mass range Ne-Fe above 10 MeV/nucleon observed on the LDEF satellite at ~470 km. Other shorter-term investigations that also took place at lower altitudes than SAMPEX have reported heavy ions above ~10 MeV/nucleon in the Earth's magnetosphere [e.g., *Tylka et al.*, 1995, and references therein].

Here we summarize over 6 years of continuous measurements from SAMPEX of the trapped, heavy ion population between L~2 and L~3 down to ~ 1 MeV/nucleon, parts of which have been reported before using SAMPEX measurements over a shorter time interval [*Selesnick et al.*, 1995b]. The low energy trapped O spectrum has been also measured down to ~4 MeV/nucleon with track detectors on Cosmos satellites [e.g., *Grigorov et al.*, 1995; *Tylka et al.*, 1996]. With the relatively long lifetime of the SAMPEX spacecraft we have been able to monitor continuously the time dependence of the trapped ACR population to much lower energies through the decline of solar cycle 22, at solar minimum, and at the rise of cycle 23. This long observation time has also been necessary in order to detect the signatures of trapped minor ACR species such as Ar, whose interplanetary abundance is <1% of ACR O.

In addition to the species with FIP above ~12 eV (O, Ne, and Ar) that were observed as interplanetary ACR, we have found a low-energy trapped component also near L~2.3 that consists of the lower FIP species C, Mg-S, and Fe. There were no features of either the spatial distributions or the time dependencies that distinguished the low-FIP from the high-FIP constituents. The origin of the trapped, lower FIP component at 1-4 MeV/nucleon is not known but might ultimately be linked to recent observations of inner heliospheric pickup ions that originate as solar wind absorbed onto interplanetary dust grains.

## 2. Observations

The observations presented here are from the SAMPEX spacecraft, launched into a 512 x 675 km, 82° inclination Earth orbit in July 1992 [*Baker et al.*, 1993]. The Low energy Ion Composition Analyzer (LICA) sensor on SAMPEX is a time-of-flight mass spectrometer [*Mason et al.*, 1993] whose energy range (~0.5–8 MeV/nucleon for $^{16}$O) overlaps with the peaks of the incident, interplanetary ACR spectra at 1 AU. The Heavy-Ion Large-area Telescope (HILT) and Mass Spectrometer Telescope (MAST) sensors also on SAMPEX [*Klecker et al.*, 1993; *Cook et al.*, 1993] cover the energies from ~8 to 45 MeV/nucleon reported here.

SAMPEX has access to trapped ACR ions near L shells of 2-3 in the weaker magnetic field region of the South Atlantic Anomaly [e.g., *Cummings et al.*, 1993; *Tylka*, 1993]. *Selesnick et al.* [1995a] and *Looper et al.* [1996] found maxima in the trapped ACR energy spectra at the energies corresponding to the geomagnetic cutoff rigidities for singly charged ACR incident from the west. For this study of low-energy trapped particle composition we selected a common energy range of 1-4 MeV/nucleon: we were able to determine energy spectra of trapped O and Ne up to the upper energy limits of the LICA instrument (~ 8 and ~ 7 MeV/nucleon, respectively). We also limited the L range from L=1.7 to L=3 in order to maximize the number of low-energy trapped ions and to minimize the background in LICA's lower-energy channels from penetrating protons in the inner zone.

### 2.1. Trapped Ion Composition L=1.7-3

Figure 1a shows the mass spectrum of 1-4 MeV/nucleon ions measured with LICA over the Earth's polar caps during a large solar energetic particle event in August 1998. Although the mass resolution of the sensor is best near 0.8 MeV/nucleon, Figure 1a shows that from 1-4 MeV/nucleon the instrument resolves the most abundant elements with a resolution of ~0.64 amu at mass 16. Figure 1b shows the mass spectrum of 1-4 MeV/nucleon trapped ions accumulated in L=1.7 to L=3 from July 1992 to December 1998. We corrected the mass spectra of Figures 1a and 1b for the instrumental efficiency of LICA (efficiencies of ~22, 55, and 100% for C, O, and Fe, respectively). Figure 1c plots the mass spectrum of 16-45 MeV/nucleon trapped ACR ions measured with the SAMPEX MAST instrument.

One outstanding difference between the trapped ion mass spectra of Figures 1b and 1c is the higher relative abundance of trapped Ar in the 1-4 MeV/nucleon sample not detected in

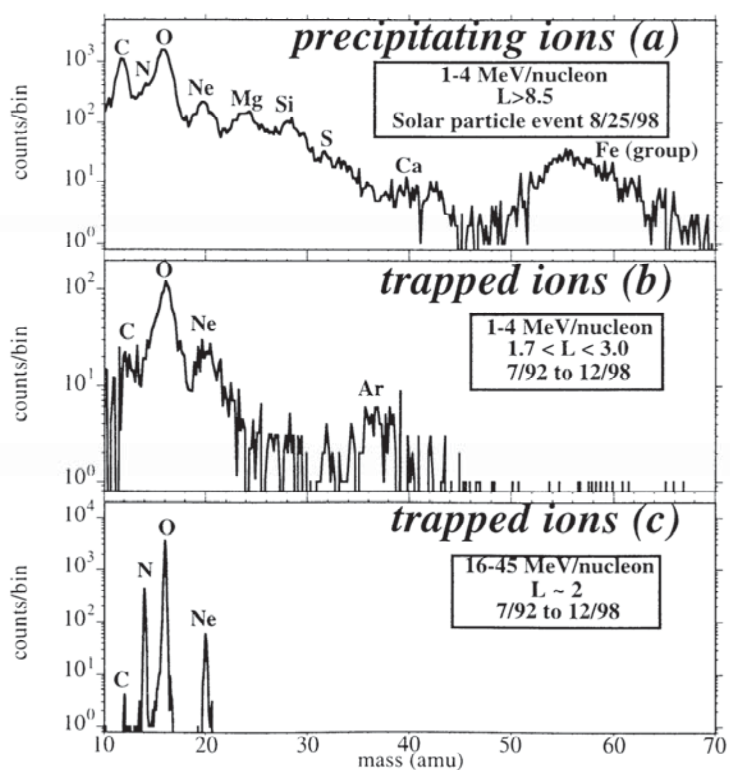


**Figure 1.** (a) Example of the mass resolution of the SAMPEX Low energy Ion Composition Analyzer in the energy range of 1-4 MeV/nucleon during a large solar energetic particle event. (b) The mass spectrum of 1-4 MeV/nucleon trapped ions from L=1.7 to L=3, accumulated for 6.5 years. (c) SAMPEX MAST mass histogram of ~ 16-45 MeV/nucleon trapped ions near L~2.

previous studies of trapped ACR above 10 MeV/nucleon (no trapped events heavier than Ne were detected with SAMPEX MAST). Compared to measurements above ~10 MeV/nucleon, this low-energy sample of the trapped particles is enhanced in C and Ne as well. Table 1 lists the relative abundances of the trapped ions at low and high energies compared with interplanetary abundances. Because of the mass resolution of the instrument in this energy range, we used a maximum likelihood technique to fit Gaussian peak shapes and a linear background to the mass spectrum of Figure 1b to derive relative abundances. We list the best fit abundance plus 1$\sigma$ for N since we observed no clear N track in this energy range.

We observed the bulk of the 1-4 MeV/nucleon trapped particles of Figure 1b near L=2.3; Figures 2a-2f show the L shell distributions for C, O, Ne, Mg-S, Ar, and Fe, respectively. The dashed curves are Gaussian fits to the measured distributions from L=1.7 to 4.0, and each plot lists the mean and standard deviation of the best fit. Each element's distribution peaked near L=2.3, and they all had similar widths in L.

### 2.2. Trapped Ion Energy Spectra

The relative abundances of the trapped ions are energy-dependent. In order to explore the energy dependence, we compare in Figure 3 the energy spectra of O, Ne, and Ar observed in the trapped radiation between L=1.7 and 3 with the spectra in interplanetary space at 1 AU. The trapped O and Ne spectra above ~10 MeV/nucleon were measured with the SAMPEX HILT sensor from August 1992 to February 1994 averaged over L=1.7 to 3.0, then scaled by a factor of 1.55 to account for the rise in the trapped ACR fluxes across the period of this study (–see Plate 1). The interplanetary O and Ne ACR spectra above ~10 MeV/nucleon were measured with the SAMPEX HILT sensor in late 1995 and have been scaled to the average flux of ~20 MeV/nucleon O and Ne also measured on SAMPEX from July 1992 to December 1998. We corrected the interplanetary O and Ne spectra below 10 MeV/nucleon for quiet time solar and interplanetary contributions by fitting the low-energy spectra below 1 MeV/nucleon with power laws. We then subtracted the best fits of power law spectra, proportional to (MeV/nucleon)$^{-2.7}$, from the measurements to derive the low-energy points shown in the interplanetary spectra of O and Ne of Figure 3. This correction was most significant for the two lowest energy points of the O and Ne spectra. We show the 1 AU quiet time Ar spectrum averaged from November 1994 to April 1998 with instrumentation on board the Wind satellite [*Reames*, 1999a] along with the interplanetary quiet time Ar flux at 1-4 MeV/nucleon from July 1992 to December 1998 measured on SAMPEX. We note that if averaged from November 1994 to April 1998, the resulting trapped Ar fluxes measured on SAMPEX were ~2 times lower than those shown in Figure 3, representing a trapped particle enhancement of a factor of ~100. Even so, the Ar spectra of Figure 3 illustrate the lower-energy peak of the trapped Ar compared to the O and Ne.

Figure 4 compares the trapped particle energy spectra of the less abundant C, Mg-S, and Fe with the spectra of the ACR species O, Ne, and Ar at ~1-4 MeV/nucleon. There is a rough mass-dependent ordering to the spectral slopes in this energy range. The power law fits in Figure 4 show the dependence; even though the fits do not fully describe the peaked Ar or Fe spectra and are shown only to illustrate the trend, they do show that higher masses tended to have the softest spectra. *Selesnick et al.* [1995a] found integral energy spectra of trapped N, O, and Ne that were also softer with larger $Z$. However, the spectra of *Selesnick et al.* [1995a] above 10 MeV/nucleon all had negative spectral slopes in contrast to the positive slopes of C through Ne in Figure 4.

### 2.3. Time Histories of Trapped Fluxes

The time dependence of the trapped fluxes is another diagnostic of their source and loss mechanisms. Plate 1a shows the time dependence of trapped O at 1-4 MeV/nucleon and near ~20 MeV/nucleon. In contrast to the relatively constant trapped flux above 20 MeV/nucleon from 1995 to early 1998 [*Selesnick et al.*, 1998], the lower energy O increased in intensity by a factor of 3 in early 1996. The low-energy trapped C, Ne, and Mg-S also reached maximum intensity near late 1996 or early 1997, and the Ar flux peaked in early 1996 (Plates 1b-1c). Plate 1d indicates that the peak intensities of the low-energy trapped ions roughly coincided with a minimum in geomagnetic activity as measured by the frequency of geomagnetic storms with minimum *Dst* indices below –75 nT. The trapped particle intensities reached their maximum when there were few interplanetary particle events associated either with interplanetary shocks or with high-speed solar wind streams (Plate 1e).

**Table 1.** Abundances of Trapped Ions Near 1 MeV/nucleon and Above 10 MeV/nucleon Compared to Interplanetary Abundances

| Element | First Ionization Potential, eV | Trapped Ions 1-4 MeV/nucleon [a] | Trapped Ions 16-45 MeV/nucleon [b,c] | Geo-magnetically Filtered $Q = 1$ [b] ~8-20 MeV/nucleon | Interplanetary Quiet Time [d] ~ 5 MeV/nucleon |
|---|---|---|---|---|---|
| C | 11.26 | 124 ± 28 | 0.8 ± 0.3 | 12.9 ± 7.1 | 7 ± 7 |
| N | 14.53 | <140 | 90 ± 10 | - | 139 ± 2 |
| O | 13.61 | 1000 ± 46 | 1000 | 1000 | 1000 ± 6 |
| Ne | 21.56 | 285 ± 21 | 30 ± 2.5 | 50 ± 4 | 74 ± 2 |
| Mg+Si+S | 7.64-10.36 | 88 ± 17 | < 2.0 | ~ 1 | 2.9 ± 1.1 |
| Ar | 15.76 | 73 ± 9 | < 1.1 | < 0.3 | 3.7 ± 0.4 |
| Fe | 7.87 | 17 ± 4 | < 2.3 | < 0.3 | 0.8 ± 0.2 |

[a]This work. L =1.7-3.
[b]*Klecker et al.* [1998].
[c]*Selesnick et al.* [1995a].
[d]*Reames* [1999a].

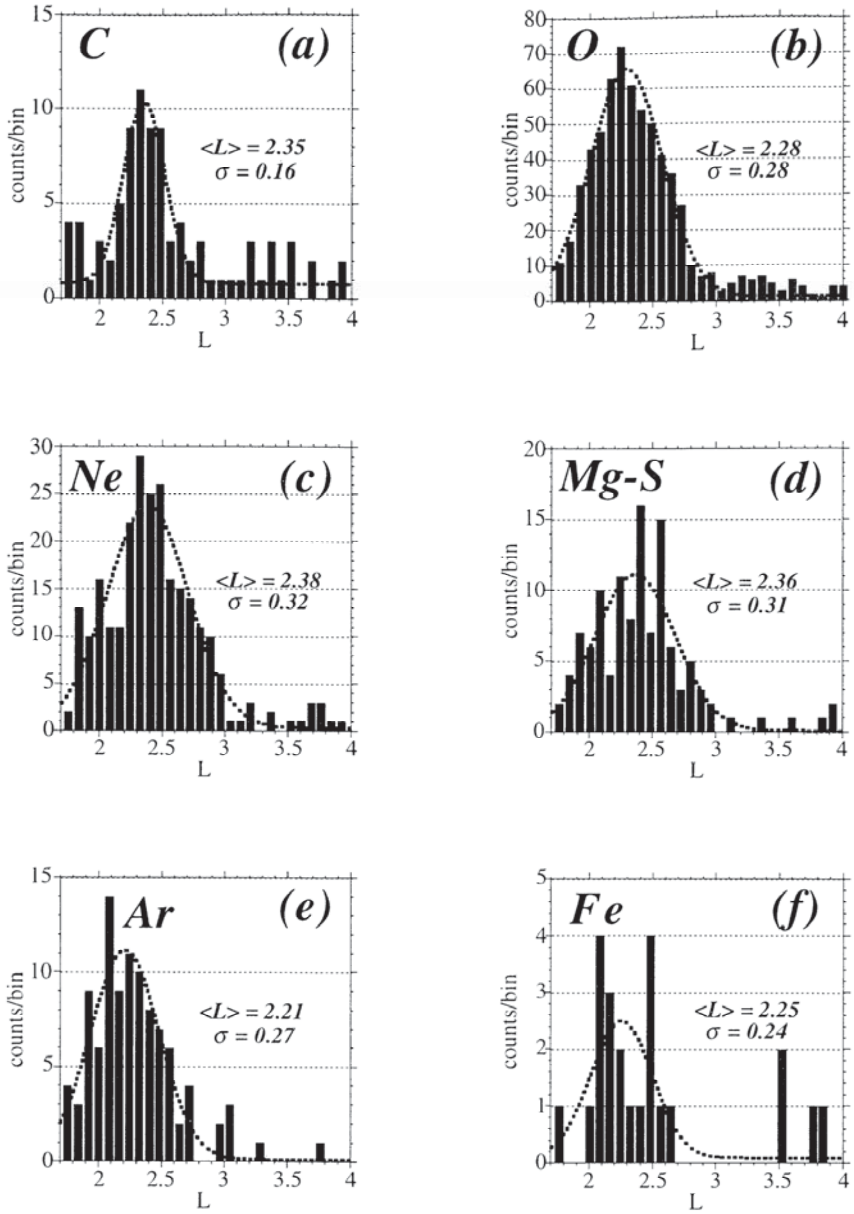


**Figure 2.** L-shell distributions of 1-4 MeV/nucleon trapped (a) C, (b) O, (c) Ne, (d) Mg-S, (e) Ar, and (f) Fe. Figures 2a-2f show the Gaussian fits to the distributions as well as the best fit mean and standard deviation.

## 3. Discussion and Conclusions

The new measurements presented here extend the continuous observations of trapped ions between L~2 and ~3 to much lower energies than were previously available. In a survey that covers the decline of solar cycle 22 through the rise of cycle 23 we found significant trapped abundances of the known ACR species O, Ne, and Ar at 1-4 MeV/nucleon. We also found traces of the low-FIP species (i.e., FIP ≤ 12 eV) C, Mg-S, and Fe at 1-4 MeV/nucleon. At these low energies all the trapped species had maximum intensities near L=2.3 with similar spatial widths in L. There were no features of the spatial distributions that distinguished one trapped species from another. The low-energy trapped ions peaked in intensity between 1996 and 1997, roughly near solar minimum. Even though we needed to create yearly sums of the rare C, Mg-S, and Fe to follow their time dependencies, we find that a continuously present source describes their arrival at SAMPEX better than discrete injections such as large solar energetic particle events. Within the uncertainties of the measurements there were no features of the time dependencies that distinguished, for example, a low-FIP element such as C from the more abundant high-FIP O.

### 3.1. ACR Species O, Ne, and Ar

We first consider the trapped O, Ne, and Ar observed down to 1 MeV/nucleon. These ions are known components of the interplanetary ACR population. At the altitude of SAMPEX the most abundant trapped heavy ions (O and Ne) below ~10 MeV/nucleon are at energies too low to have had direct access as singly ionized incident ACR. Figure 5 shows that the western cutoff energies [*Smart and Shea*, 1993] of singly charged O and Ne are >4 MeV/nucleon for the range of L shells of this study. Near the South Atlantic Anomaly the Earth's magnetic field will

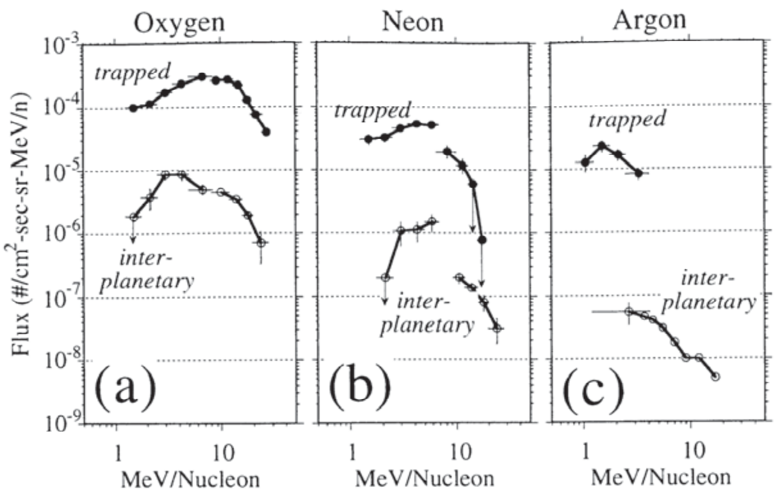


**Figure 3.** Comparison of the trapped and interplanetary O, Ne, and Ar energy spectra.

deflect singly charged ions from the east that graze the atmosphere into the lower atmosphere where they will become lost. We therefore compare these measurements with the minimum energy for singly ionized ions that arrive from the west, deriving the western cutoff energies from the western cutoff rigidity under the assumption of singly charged incident ions. We note that the trapped O and Ne above ~10 MeV/nucleon have been observed at lower L shells [e.g., *Selesnick et al.*, 1995a], consistent with the cutoff energy curves shown in Figure 5. In order to observe trapped O and Ne at lower energies we suggest that the higher-energy ions have been degraded in energy during their confinement within the magnetosphere. Indeed, the energy spectra of the trapped O and Ne level off below a few MeV/nucleon as expected because of the energy loss of higher-energy trapped ions in the residual atmosphere [*Blake*, 1990].

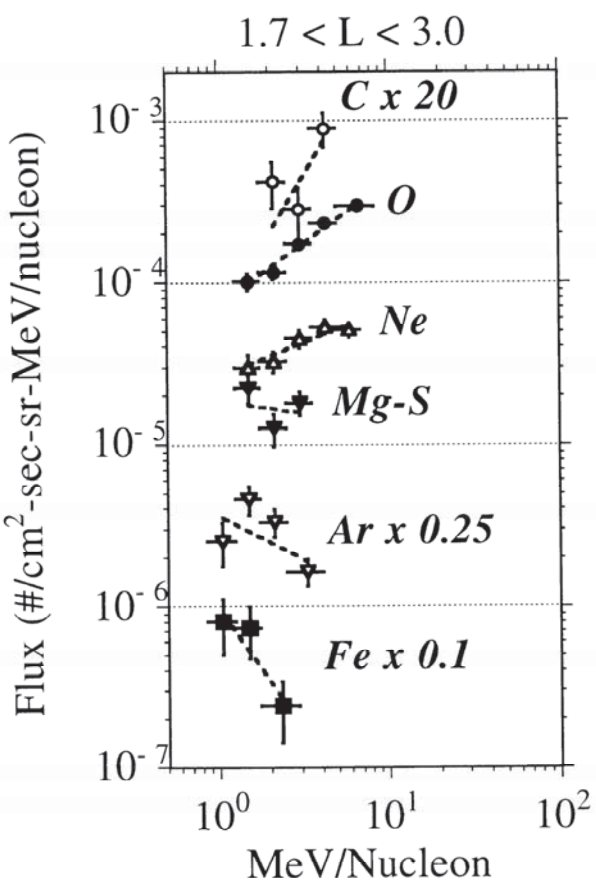


**Figure 4.** Comparison of trapped ion energy spectra between ~1 and ~8 MeV/nucleon measured with SAMPEX LICA. The dashed lines are power law fits to the data points.

Several factors have contributed to the higher relative abundance of Ar in the 1-4 MeV/nucleon trapped population. Peak intensities of interplanetary ACR ions occur at energies inversely proportional to the particle mass [e.g., *Cummings and Stone*, 1995]. The interplanetary energy spectra of Figure 3 indicate a lower energy peak for Ne and Ar compared to O, and these peaks lie well below the ~16 MeV/nucleon threshold of the previous studies by *Klecker et al.* [1998] and *Selesnick et al.* [1995a]. Table 2 lists the energies of peak ACR intensity measured in the distant heliosphere [*Cummings and Stone*, 1995]; these are consistent with the peak energies observed at 1 AU (-see Figure 3).

It is also the case that the cutoff energy for singly charged Ar is within the 1-4 MeV/nucleon energy range (Figure 5). We observed a spectral peak in the trapped Ar between 1 and 2 MeV/nucleon that is near the western cutoff energy for $Ar^{+1}$. The lower energy of the Ar peak compared to those of O and Ne shown in Figure 3 is qualitatively consistent with calculations by *Tylka* [1993] and suggests that at 1-4 MeV/nucleon the interplanetary Ar is mostly singly ionized. We would expect lower-energy interplanetary Ar to be mostly singly ionized on the basis of the observation that the energy per nucleon below which interplanetary ACR N, O, and Ne are mostly singly ionized decreases with increasing mass [e.g., *Klecker et al.*, 1998]. The expected flattening of the trapped Ar spectrum due to energy loss lies below the 1 MeV/nucleon threshold of this study.

Finally, Table 2 compares the equilibrium charge states of O, Ne, and Ar [*Johnson*, 1990] at the peak interplanetary intensities. The equilibrium charge state is a measure of the possible average charge state an ACR ion acquires upon passage through some of the residual atmosphere. The details of the trapping process are complex and depend on geomagnetic access and adiabatic motion after ionization in the atmosphere [e.g., *Tylka*, 1994; *Selesnick et al.*, 1995a]. However, assuming the ions are singly ionized before becoming trapped, Table 2 suggests that the change in the

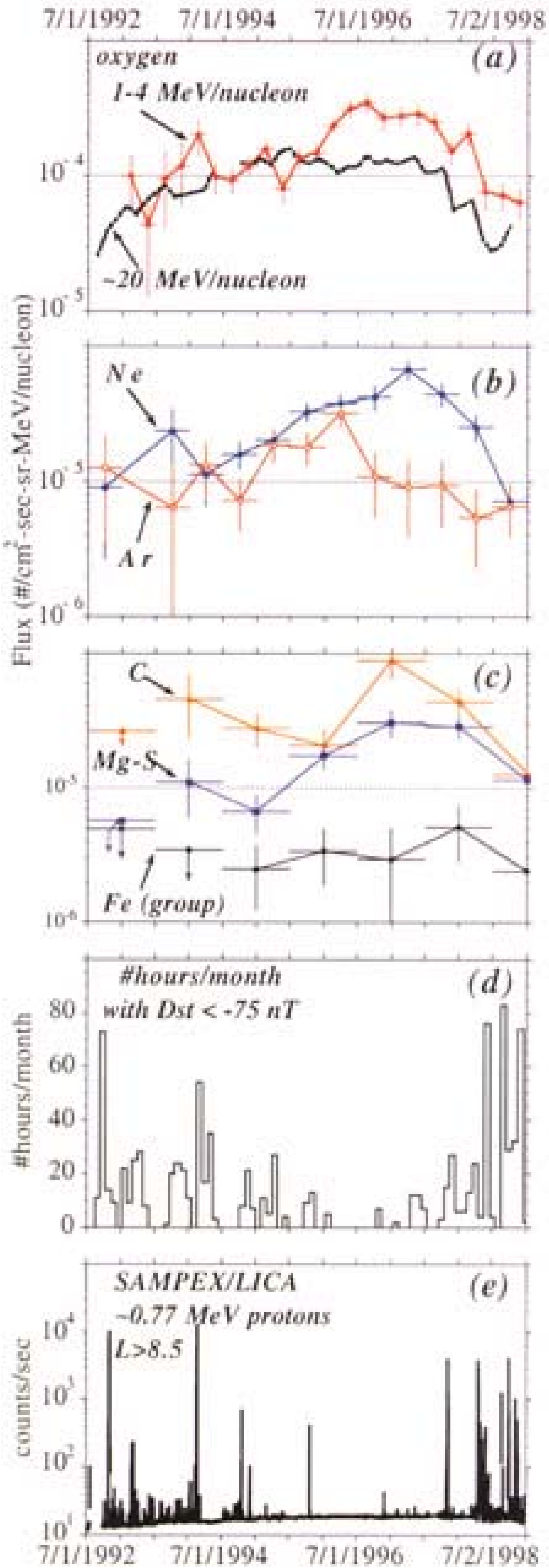


**Plate 1.** (a) Time dependence of trapped anomalous cosmic ray (ACR) O at 1-4 MeV/nucleon and ~20 MeV/nucleon from July 1992 to December 1998. (b)-(c) Longer-term averages of trapped 1-4 MeV/nucleon Ne, Ar, C, Mg-S, and Fe. (d) Histogram of the number of hours per month wherein the *Dst* index was below −75 nT. (e) Daily averaged count rate of >0.77 MeV ions (mostly protons) observed in interplanetary space.

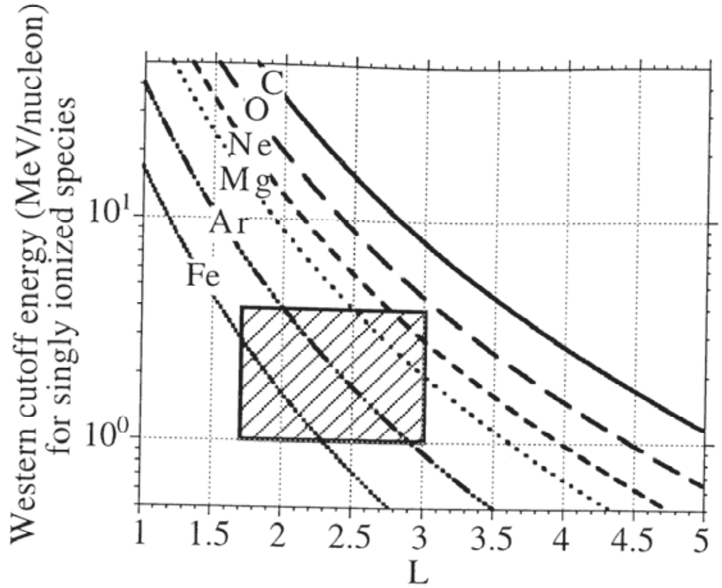


**Figure 5.** Western cutoff energies of singly charged C, O, Ne, Mg, Ar, and Fe as functions of L shell [*Smart and Shea*, 1993]. The hatched box shows the L range and energy range for the low energy trapped particle composition portion of this work.

ionization state of Ar is greatest (Ar loses ~12 electrons compared to a loss of ~6 for O). The Ar may then be more likely to obtain an adiabatic motion once stripped to its equilibrium charge state and therefore may be more likely to become stably trapped.

The fluxes of the trapped ACR O and Ne are enhanced relative to the interplanetary fluxes by factors of ~50-100 depending on energy. This first measurement of the trapped Ar spectrum shows that the enhancement factor is roughly 100 at ~3.5 MeV/nucleon where there is overlap between the trapped and interplanetary Ar spectra.

### 3.2. Trapped C

We next consider the trapped C observed down to 1 MeV/nucleon. We may suppose that the same mechanism of energy loss in the residual atmosphere that explains the low-energy O and Ne also accounts for the low-energy C. Indeed, above 16 MeV/nucleon the trapped C/O ratio is ~0.0008 [*Klecker et al.*, 1998] (see also Figure 1c), so there is a population of higher-energy C that might degrade in energy and eventually pass through the 1-4 MeV/nucleon interval. However, if the O spectrum is softer than that of C [*Selesnick et al.*, 1995a], then the C/O ratio toward lower energies would be lower than 0.0008. The details of the trapped C lifetime might then have to account for the factor of ~150 increase in the C/O abundance at lower energies. In fact, the low-energy trapped population has a larger C/O ratio compared to the interplanetary singly ionized population at 8-20 MeV/nucleon as well as the quiet time interplanetary abundances at 5 MeV/nucleon (Table 1).

*Hovestadt et al.* [1978, 1981] measured the heavy ion composition of the radiation belts above L~2.5 during perigee passes of the ISEE 1 spacecraft. They found significant fluxes of C, O, and Ne-Si below ~1 MeV/nucleon with peaks in the trapped C and O fluxes near L=3. The trend they observed for the peak intensity to move inward to lower L with increasing energy might suggest that we have observed at least a portion of the same population in this survey. However, *Hovestadt et al.* [1981] found C/O as high as ~4 at 1.2 MeV/nucleon, nearly a factor of 10 higher than that observed with SAMPEX between 1and 4 MeV/nucleon.

Turning to the energy spectra of Figure 4, we note that the C and Mg-S spectra may have additional components that increase in intensity below 1 MeV/nucleon. If extrapolated to lower energies, a power law fit to the two lowest-energy C points in Figure 4 intersects the O spectrum near ~0.85 MeV/nucleon, although with considerable uncertainty. There is therefore a possibility that the trapped population observed by *Hovestadt et al.* [1978, 1981] exists in these measurements as well, although at much lower energies.

**Table 2.** Equilibrium Charge States of ACR Ions Upon Traversal of Residual Atmosphere

| Element | Energy/nucleon at peak intensity of ACR spectrum, MeV/nucleon[a] | Equilibrium charge state at peak intensity $Z^*$ [b] | Change in ionization state: $Z^* - Q_0$ [c] |
|---|---|---|---|
| O | 4.2 | 7.3 | 6.3 |
| Ne | 3.0 | 8.8 | 7.8 |
| Ar | 1.4 | 13.1 | 12.1 |

[a]Peak intensity of ACR energy spectra measured at Voyager 2 in 1994 [*Cummings and Stone*, 1995].
[b]Equilibrium charge states from *Johnson* [1990].
[c]Change in ACR ionization state assuming initially singly ionized particles ($Q_0 = 1$).

### 3.3. Observations of Rare, Interplanetary ACR Species

*Reames* [1999a] found spectral turn-ups in the interplanetary Mg, Si, and S at 1 AU that were significantly above the quiet time levels of these species, but only below ~5 MeV/nucleon. If these Mg, Si, and S were singly charged, then the combination of low-energy spectral increases, western cutoff energies well below

10 MeV/nucleon, and the *Blake and Friesen* [1977] trapping process may then account for their presence only in the low-energy trapped population.

If the trapped, 1-4 MeV/nucleon Mg-S is linked to an energetic, interplanetary, and singly ionized component of these ions, then we can ask whether the trapped C and Fe also have corresponding interplanetary signatures. *Reames* [1999a] did not observe significant turn-ups in the quiet time spectra of C or Fe near ~5 MeV/nucleon at 1 AU. *Stone and Cummings* [1997] did report an ACR-like enhancement of ~6-20 MeV/nucleon Fe in the outer heliosphere. The 1 AU C spectral increase observed in 1992-1993 [*Mewaldt et al.*, 1993] may have been dominated by higher charge state C. There is therefore a considerable variety of observations of interplanetary energetic ions that may be relevant to the trapped population of this study, although these interplanetary measurements were made at energies above the 1-4 MeV/nucleon interval considered here.

### 3.4. Low-Energy Trapped Ions Ordered by FIP

Even though the elements in the low-energy trapped population had similar spatial and time dependencies, it is the case that their abundances differed when compared to the solar wind. Figure 6 shows the relative abundances of 1-4 MeV/nucleon trapped ions as a function of FIP. Here the normalizing element is C rather than O because we want to address the rare, lower FIP species as a group. The solid symbols are the in-ecliptic, slow solar wind abundances [*von Steiger and Geiss*, 1997]. We added the Mg, Si, and S abundances and plotted the results at the average FIP of these species. While the more abundant trapped species N, O, Ne, and Ar that are also found in the interplanetary ACR component are enhanced compared to the solar wind by amounts that increase with increasing mass, the trapped species below ~12 eV have roughly solar wind abundances. *Reames* [1999b] showed that FIP is a natural means of distinguishing the ACR species O, Ne, and Ar from species with lower FIP; the O, Ne, and Ar are mostly neutral in the interstellar medium and are therefore not filtered out by the magnetic fields in the outer heliosphere. Following this idea, Figure 6 implies that the low-energy trapped population might be a mixture of the high-FIP ACR species N, O, Ne, and Ar and lower-FIP species with roughly solar wind abundances (C, Mg-S, and Fe). Indeed, we cannot rule out the possible contribution of a solar-like source to the high-FIP constituents as well. We note that a comparison of the trapped particle composition with solar energetic particle abundances would yield a similar result.

There are several observations of trapped energetic ions that also place the results of this study into a broader context. The lower-energy portions of the trapped C and Mg-S spectra reported here may indicate that at much lower energies a magnetospheric source contributes to the trapped population between L~2 and ~3. *Hovestadt et al.* [1978] suggested that this population originates as solar wind that is accelerated in geomagnetic storms and then radially diffused inward. However, on the basis of the energy spectra measured on ISEE 1 the bulk of this possible source is well below the 1 MeV/nucleon threshold of this study.

It is also the case that interplanetary shock compression of the magnetosphere can indirectly inject ambient solar energetic protons onto trapped trajectories below L~4 [e.g., *Hudson et al.*, 1997]. The injection events that *Hudson et al.* [1997] reported occurred during solar maximum in 1991. Because this mechanism requires a seed population of solar energetic particles, we would expect fewer injection events in 1996 when the trapped 1-4 MeV/nucleon flux reached its maximum intensity. It is unknown how in detail the trapped particles of this study may relate to the shock injection mechanism; we mention it here because it is an observed means of creating new, trapped populations at low values of L.

Recent measurements of pickup ions from an inner-heliospheric source [e.g., *Geiss et al.*, 1995] may also be relevant to the question of the ultimate source of the trapped energetic population. *Geiss et al.* [1995] identified an inner heliospheric source of pick-up ion $C^{+1}$ that they attributed to interstellar dust. *Fahr and Ripken* [1985] discussed interplanetary neutrals that originate from solar wind absorbed onto interplanetary dust grains, and it is possible that other pickup ions observed on the Ulysses spacecraft within ~3 AU of the sun (H, N, O, Ne, Mg, and Si) originate from this source [*Gloeckler et al.*, 2000]. To what extent these pickup ions participate in the ACR acceleration process just as the more abundant, high FIP interstellar ions in order to contribute to the low energy trapped population via the *Blake and Friesen* [1977] process is uncertain.

We have found that the 1-4 MeV/nucleon trapped particle population has a rich variety of potential sources. Even so, the time dependence and spatial locations of the low-FIP and high-FIP trapped ions show that their similarities outweigh their differences. Their spectra shapes also suggest a common ordering, perhaps by western cutoff rigidity. We expect that

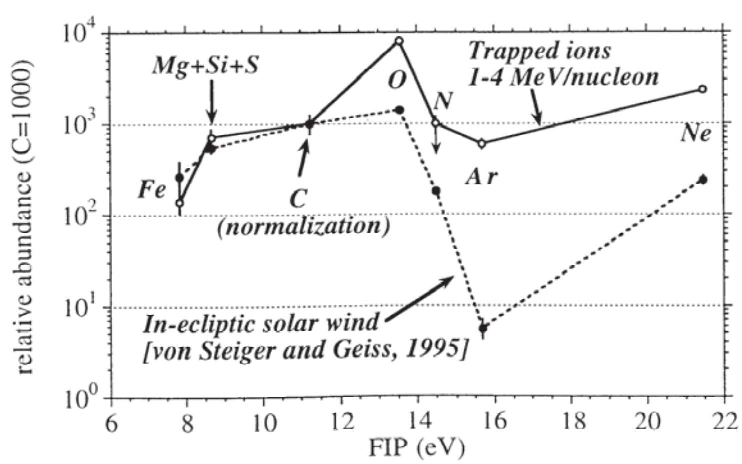


**Figure 6.** The 1-4 MeV/nucleon trapped ion abundances normalized to C (open symbols) compared to in-ecliptic solar wind (solid symbols) versus first ionization potential.

continued observations of perturbations of the 1-4 MeV/nucleon trapped population with SAMPEX through the upcoming solar maximum will shed further light on the processes that create and degrade the belt of low energy heavy ions near L~2.3. Modeling of the *Blake and Friesen* [1977] process using a particle propagation code (M. C. McNab, personal communication, 1999) that includes particle stripping and energy loss will also shed light on the trapped particle lifetime and the trapping efficiencies for the rare Mg-S and Fe species.

Acknowledgments. We thank the members of the SAMPEX instrument teams who have contributed to the success of the SAMPEX mission as well as the personnel at the Goddard Space Flight Center who constructed, launched, and operate the SAMPEX spacecraft. We also thank R. S. Selesnick for helpful discussions and for providing the time history of the trapped ACR oxygen at 20 MeV/nucleon. The cooperative agreement Z628302 between the University of Maryland and The Aerospace Corporation, funded through NASA grant NAG5-2963, supported this work.

Janet G. Luhmann thanks Rudolph von Steiger and Allan J. Tylka for their assistance in evaluating this paper.

## References

Baker, D. N., G. M. Mason, O. Figueora, G. Colon, J. G. Watzin, and R. M. Aleman, An overview of the Solar, Anomalous, and Magnetospheric Particle Explorer (SAMPEX) mission, *IEEE Trans. Geosci. Remote Sens.*, *31*, 531-541, 1993.

Barz, S., R. Beaujean, and W. Enge, Trapped oxygen and neon measurements on LDEF, *Proc. 24th Int. Cosmic Ray Conf.*, *4*, 1009-1012, 1995.

Blake, J. B., Geomagnetically trapped heavy ions from anomalous cosmic rays, *Proc. 21st Int. Cosmic Ray Conf.*, *7*, 30-33, 1990.

Blake, J. B., and L. M. Friesen, A technique to determine the charge state of the anomalous low-energy cosmic rays, *Proc. 15th Int. Cosmic Ray Conf.*, *2*, 341-346, 1977.

Cook, W. R., A. C. Cummings, J. R. Cummings, T. L. Garrard, B. Kecman, R. A. Mewaldt, R. S. Selesnick, E. C. Stone, and T. T. von Rosenvinge, MAST: A mass spectrometer telescope for studies of the isotopic composition of solar, anomalous, and galactic cosmic ray nuclei, *IEEE Trans. Geosci. Remote Sens.*, *31*, 557-564, 1993.

Cummings, A. C., and E. C. Stone, Elemental composition of the anomalous cosmic ray component, *Proc. 24th Int. Cosmic Ray Conf.*, *4*,497-500, 1995.

Cummings, J. R., A. C. Cummings, R. A. Mewaldt, R. S. Selesnick, E. C. Stone, and T. T. von Rosenvinge, New evidence for geomagnetically trapped anomalous cosmic rays, *Geophys. Res. Lett.*, 20, 2003-2006, 1993.

Fahr, H. J., and H. W. Ripken, Dust-plasma interactions in the heliosphere, in *Properties and Interactions of Interplanetary Dust*, edited by R. H. Giese and P. Lamy, pp. 305-323, D. Reidel, Norwell, Mass., 1985.

Geiss, J., G. Gloeckler, L. A. Fisk, and R. von Steiger, C+ pickup ions in the heliosphere and their origin, *J. Geophys. Res.*, *100*, 23,373-23,377, 1995.

Gloeckler, G., L. A. Fisk, J. Geiss, N. A. Schwadron, and T. H. Zurbuchen, Elemental composition of the inner source pickup ions, *J. Geophys. Res.*, *105*, 7459-7463, 2000.

Grigorov, N. L., M. A. Kondratyeva, M. I. Panasyuk, C. A. Tretyakova, J. H. Adams, J. B. Blake, M. Shultz, R. A. Mewaldt, and A. J. Tylka, Evidence for trapped anomalous cosmic ray oxygen ions in the inner magnetosphere, *Geophys. Res. Lett.*, *18*, 1959-1962, 1991.

Grigorov, N. L., M. A. Kondratyeva, M. I. Panasyuk, C. A. Tretyakova, S. P. Tretyakova, and D. A. Zhuravlev, The energy spectra of interplanetary and trapped anomalous cosmic rays, *Proc. 24th Int. Cosmic Ray Conf.*, *4*, 1025-1028, 1995.

Hovestadt, D., G. Gloeckler, C. Y. Fan, L. A. Fisk, F. M. Ipavich, B. Klecker, J. J. O'Gallagher, and M. Scholer, Evidence for solar wind origin of energetic heavy ions in the Earth's radiation belt, *Geophys. Res. Lett.*, *5*, 1055-1057, 1978.

Hovestadt, D., B. Klecker, E. Mitchell, J. F. Fennell, G. Gloeckler, and C. Y. Fan, Spatial distribution of Z≥2 ions in the outer radiation belt during quiet conditions, *Adv. Space Res.*, *1* (2), 305-308, 1981.

Hudson, M. K., S. R. Elkington, J. G. Lyon, V. A. Marchenko, I. Roth, M. Temerin, J. B. Blake, M. S. Gussenhoven, and J. R. Wygant, Simulations of radiation belt formation during storm sudden commencements, *J. Geophys. Res.*, *102*, 14,087-14,102, 1997.

Johnson, R. E., *Energetic Charged-Particle Interactions With Atmospheres and Surfaces*, Springer-Verlag, New York, 1990.

Klecker, B., D. Hovestadt, M. Scholer, H. Arbinger, M. Ertl, H. Kästle, E. Künneth, P. Laeverenz, E. Seidenschwang, J. B. Blake, N. Katz, and D. Mabry, HILT: A heavy ion large area proportional counter telescope for solar and anomalous cosmic rays, *IEEE Trans. Geosci. Remote Sens.*, *31*, 542-548, 1993.

Klecker, B., M. C. McNab, J. B. Blake, D. C. Hamilton, D. Hovestadt, H. Kästle, M. D. Looper, G. M. Mason, J. E. Mazur, and M. Scholer, Charge states of anomalous cosmic-ray nitrogen, oxygen, and neon: SAMPEX observations, *Astrophys. J. Lett.*, *442*, L69-L72, 1995.

Klecker, B., et al., Anomalous cosmic rays, *Space Sci. Rev.*, *83*, 259-308, 1998.

Kleis, T., A. J. Tylka, J. H. Adams Jr., L. P. Beahm, P. R. Boberg, R. Beaujean, S. Barz, & W. Enge, Trapped low-energy heavy ions results from LDEF, *Proc. 24th Int. Cosmic Ray Conf.*, *4*, 481-484, 1995.

Looper, M. D., J. B. Blake, B. Klecker, and D. Hovestadt, Trapped anomalous cosmic rays near the geomagnetic cutoff, *J. Geophys. Res.*, *101*, 24,747-24,753, 1996.

Mason, G. M., D. C. Hamilton, P. H. Walpole, K. F. Heuerman, T. L. James, M. H. Lennard, and J. E. Mazur, LEICA: A low energy ion composition analyzer for the study of solar and magnetospheric heavy ions *IEEE Trans. Geosci. Remote Sens.*, *31*, 549-556, 1993.

Mewaldt, R. A., et al., The return of the anomalous cosmic rays to 1 AU in 1992, *Geophys. Res. Lett.*, *20*, 2263-2266, 1993.

Reames, D. V., Quiet-time spectra and abundances of energetic particles during the 1996 solar minimum, *Astrophys. J.*, *518*, 473-479, 1999a.

Reames, D. V., Particle acceleration at the sun and in the heliosphere, *Space Sci. Rev.*, *90*, 413-491, 1999b.

Selesnick, R. S., A. C. Cummings, J. R. Cummings, R. A. Mewaldt, E. C. Stone, and T. T. von Rosenvinge, Geomagnetically trapped anomalous cosmic rays, *J. Geophys. Res.*, *100*, 9503-9518, 1995a.

Selesnick, R. S., R. A. Mewaldt, E. C. Stone, G. M. Mason, J. E. Mazur, J. B. Blake, B. Klecker, and D. Hovestadt, Observations of geomagnetically trapped anomalous cosmic rays, *Proc. 24th Int. Cosmic Ray Conf.*, *4*, 1013-1016, 1995b.

Selesnick, R. S., R. A. Mewaldt, and R. A. Leske, Solar-cycle effects on the intensity of high energy heavy ions in Earth's radiation belts, *EOS Trans. AGU*, *79*, (45), Fall Meet. Suppl., F756, 1998.

Smart, D. F., and M. A. Shea, The change in geomagnetic cutoffs due to changes in the dipole equivalent of the Earth's magnetic field, *Proc. 23rd Int. Cosmic Ray Conf.*, *3*, 781-784, 1993.

Stone, E. C., and A. C. Cummings, Evidence for anomalous cosmic ray S, Si, and Fe in the outer heliosphere and for a non-ACR source of S at 1 AU, *Proc. 25th Int. Cosmic Ray Conf.*, *2*, 289-292, 1997.

Tylka, A. J., Spectra and geographical distribution of geomagnetically trapped anomalous cosmic rays, *Proc. 23rd Int. Cosmic Ray Conf.*, *3*, 436-439, 1993.

Tylka, A. J., Theoretical modeling and interpretation of trapped anomalous cosmic rays, *Proc. 23rd Int. Cosmic Ray Conf., Invited, Rapporteur, and Highlight Papers*, edited by D. A. Leahy, R. B. Hicks, and D. Venkatesan, pp. 436-439, *World Scientific, Singapore*, 1994.

Tylka, A. J., P. R. Boberg, J. H. Adams Jr., T. Kleis, and R. Beaujean, On purported observations of partially ionized galactic cosmic rays, *Astrophys. J. Lett.*, *438*, L83-L86, 1995.

Tylka, A. J., P. R. Boberg, & J. H. Adams Jr., LET spectra of trapped anomalous cosmic rays in low-earth orbit, *Adv. Space Res.*, *17* (2), 247-251, 1996.

von Steiger, R. and J. Geiss, Composition of the solar wind, in *Cosmic Winds and the Heliosphere*, edited by J. R. Jokipii, C. P. Sonett, and M. S. Giampapa, pp. 581-616, Univ. Ariz. Press, Tuscon, 1997.

J. B. Blake, M. D. Looper, and J. E. Mazur, Space Sciences Department, The Aerospace Corporation, 2350 E. El Segundo Blvd., El Segundo, CA 90245.

B. Klecker, Max-Planck-Institut für Extraterrestriche Physik, Garching, Germany D-87540.

R. A. Leske and R. A. Mewaldt, Department of Physics, California Institute of Technology, Pasadena, CA 91125.

G. M. Mason, Department of Physics, University of Maryland, College Park, MD 20742.

(Received July 22, 1999; revised December 13, 1999; accepted December 20, 1999.)